

NANO EXPRESS

Open Access



Theoretical and Experimental Study on AlGa_N/Ga_N Schottky Barrier Diode on Si Substrate with Double-Heterojunction

Tao Sun, Xiaorong Luo^{*} , Jie Wei, Chao Yang and Bo Zhang

Abstract

An AlGa_N/Ga_N Schottky barrier diode (SBD) with double-heterojunction is theoretically and experimentally investigated on the Ga_N/AlGa_N/Ga_N/Si-sub. The two-dimensional hole gas (2DHG) and electron gas (2DEG) are formed at the Ga_N-top/AlGa_N and AlGa_N/Ga_N interface, respectively. At the off-state, the 2DEH and 2DHG are partially depleted and then completely disappear. There remain the fixed positive and negative polarization charges, forming the polarization junction. Therefore, a flat electric field in the drift region and a high breakdown voltage (BV) are obtained. Moreover, the anode is recessed to reduce turn-on voltage (V_{ON}). The low-damage ICP etching process results in the improved Schottky contacts, and a low leakage current and a low V_{ON} is obtained. The fabricated SBD exhibits a BV of 1109 V with anode-to-cathode distance (L_{AC}) of 11 μm . The fabricated SBDs achieve a low V_{ON} of 0.68 V with good uniformity, a high on/off current ratio $\sim 10^{10}$ at room temperature, a low specific on-resistance ($R_{ON,SP}$) of 1.17 $\text{m}\Omega \text{cm}^2$, and a high Baliga's figure-of-merit (FOM) of 1051 MW/cm^2 .

Keywords: Ga_N, Schottky barrier diode (SBD), Breakdown voltage, Silicon substrate

Introduction

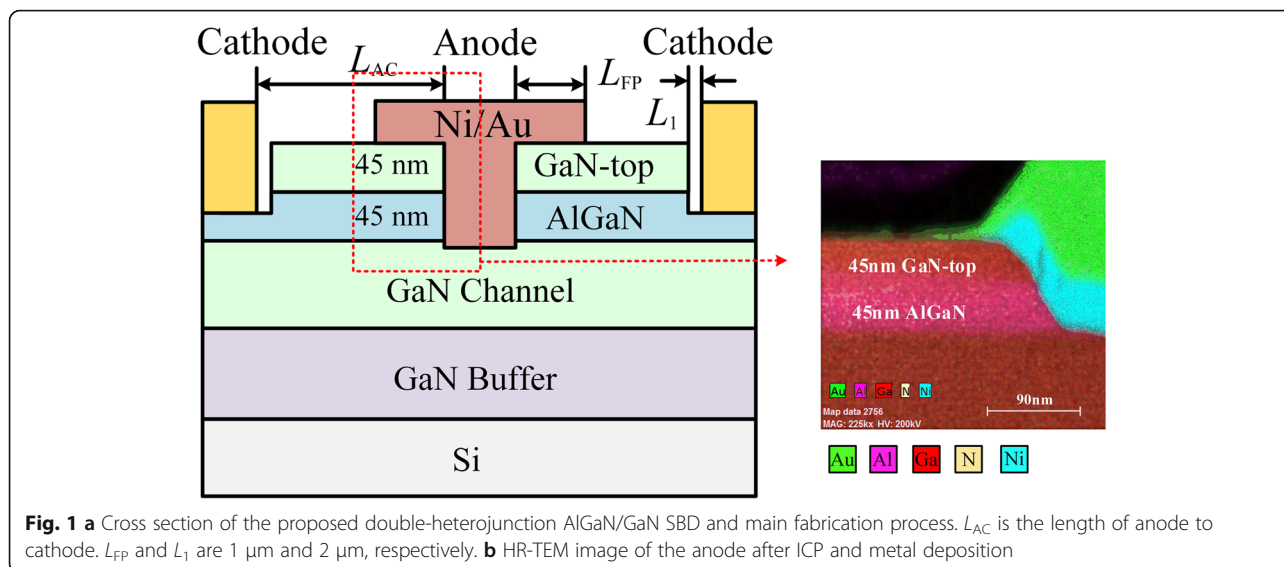
AlGa_N/Ga_N heterostructure-based lateral diode is an attractive device because of the high electron mobility of the two-dimensional electron gas (2DEG), high electron saturation velocity, and high breakdown electric field [1–3]. Extensive efforts have been made to achieve a low turn-on voltage (V_{ON}), a low reverse leakage current and a high breakdown voltage (BV) for the Ga_N diodes used in converters and inverters for power supplies and power factor corrections [4–12]. Various approaches have been proposed to solve the non-uniform distribution of the electric field. One of them is the field-plate (FP) technology [5, 13]. A fully recessed anode SBD with a dual field plate achieves a high breakdown voltage of 1.9 kV with 25 μm L_{AC} [5]. It can also significantly reduce turn-on voltage while maintaining high breakdown voltage. In addition, the conventional

Reduced Surface Field (RESURF) concept commonly employed in silicon technology has been demonstrated in Ga_N HEMT [14]. Moreover, the polarization junction (PJ) consisting of the two-dimensional hole gas (2DHG) above the 2DEG is proposed to improve the relationship between specific on-resistance ($R_{ON,SP}$) and BV [15–18]. Ga_N-based devices based on the PJ concept have been demonstrated on Sapphire and SiC substrate, while the high cost and small diameters of the Ga_N on SiC substrates go against the mass commercial application. Ga_N-on-Si with a large diameter is considered as a promising choice owing to the low cost [19–22]. Therefore, the performance of the PJ diode on silicon substrates is worthy of study.

In this work, we proposed and experimentally demonstrated a Ga_N/AlGa_N/Ga_N-on-Si Schottky barrier diode with double-heterojunction (DJ). The polarization-junction effect is confirmed by simulations and experiments. The flat electric field (E-field) between the anode and cathode electrodes is achieved. The ICP process to etch Schottky trench is optimized to achieve a low reverse

* Correspondence: xrluo@uestc.edu.cn

State Key Laboratory of Electronic Thin Films and Integrated Devices, University of Electronic Science and Technology of China, Chengdu 610054, China

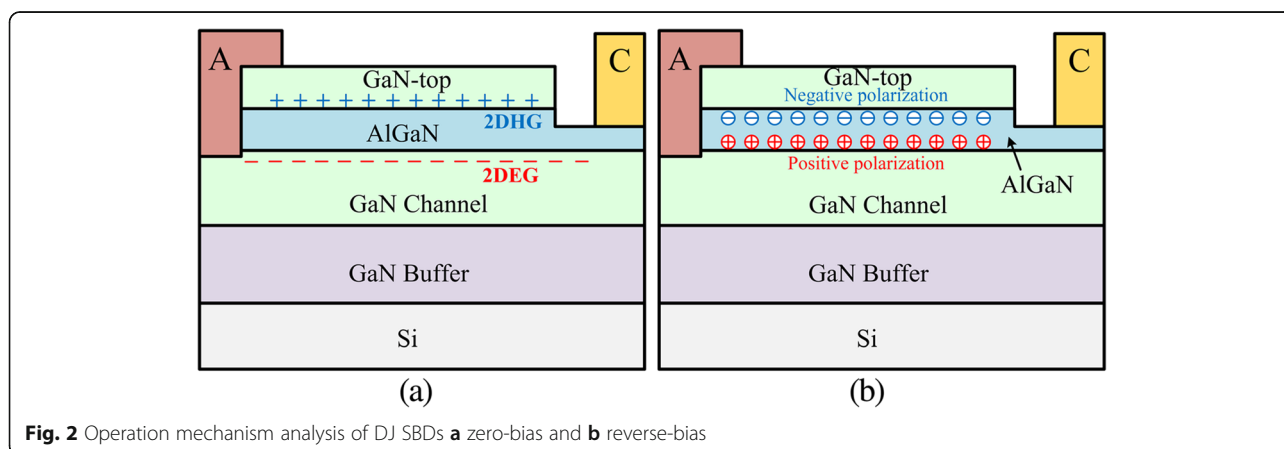


leakage current and a low V_{ON} with excellent etching uniformity. The ohmic contact process is also optimized to achieve a low contact resistance (for 2DEG) based on the customized epitaxial layer (with 45 nm GaN-top). Therefore, a breakdown voltage of 1109 V is achieved for the SBDs with 11 μm L_{AC} and Baliga's figure-of-merit (FOM) is 1051 MW/cm^2 . The temperature dependence and dynamic $R_{ON,SP}$ performance are also investigated.

Method and Experiment

The epitaxial layer was grown by metal-organic chemical vapor deposition on 6-in p-type silicon, consisting of 3.5- μm GaN buffer layer, 150-nm GaN channel layer, 1-nm AlN interlayer, 45-nm $\text{Al}_{0.25}\text{Ga}_{0.75}\text{N}$ barrier layer, and 45-nm GaN-top layer from bottom to the top. The GaN-top layer includes 35-nm p-GaN layer and 10-nm undoped GaN layer. For a given AlGaIn thickness of 45 nm, the 2DHG density increases with the increase in

GaN-top thickness [22]. The thick GaN-top layer is vital to the high-density 2DHG, while it goes against the low ohmic contact resistance (for 2DEG). The schematic views of the proposed double-heterojunction Schottky barrier diode (DJ SBD) are shown in Fig. 1a. The SBD fabrication started with the mesa isolation by Cl_2/BCl_3 -based inductively coupled plasma (ICP) etching to a depth of 300 nm. Then, the ohmic trench and the Schottky anode trench were formed with the low-damage ICP etching process. The depth of the ohmic trench and the Schottky anode trench was 50 nm and 90 nm, respectively, which was confirmed by using atomic force microscopy (AFM). Tetramethylammonium hydroxide (TMAH) solution at 85 $^\circ\text{C}$ for 15 min was introduced to remove the post-etching residues and to modify the trench sidewall after finishing the etching process [23]. Then, the annealing at 400 $^\circ\text{C}$ for 10 min in N_2 ambient was carried out.



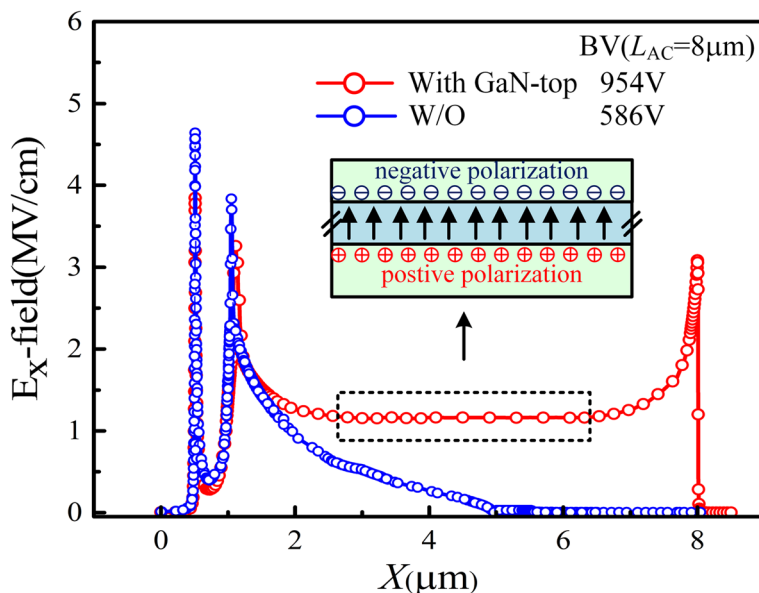


Fig. 3 Electric field distribution along the AlGaIn/GaN channel heterointerface by TCAD simulation. The Al fraction is defined as 0.25. The net acceptor (deep level) density in the buffer layer is set to be $1.5 \times 10^{16} \text{ cm}^{-3}$ and the energy level is 0.45 eV below the conduction band minimum. The acceptor density of the AlGaIn/GaN interface is set to be $6 \times 10^{12} \text{ cm}^{-3}$ and the energy level is 0.23 eV below the conduction band minimum

The ohmic cathode was subsequently formed by e-beam evaporated Ti/Al/Ni/Au (20/140/55/45 nm), annealed at 870 °C for 35 s in N₂ ambient, with a contact resistance (R_C) of 0.49 Ω·mm. Finally, anode metal and the interconnections were deposited by Ni/Au to complete the fabrication flow. The devices featured various L_{AC} from 7 to 11 μm. Figure 1b shows the high-resolution cross-section TEM image of the anode after ICP and metal deposition, and the layer structure was observed clearly.

The 2DEG is induced by the positive polarization charges along the AlGaIn/GaN interface. The upper GaN/AlGaIn interface has negative polarization charges and hence generates 2DHG at the upper interface [15]. The gap between the drift region and the cathode (L_1) is used to cut down the hole current path as shown in Fig. 2. We have only investigated the influence of L_1 from 2 to 3 μm on the forward and reverse blocking characteristics due to the limit of the original layout design. The V_{ON} and $R_{ON,SP}$ show no change because L_1 does not affect the

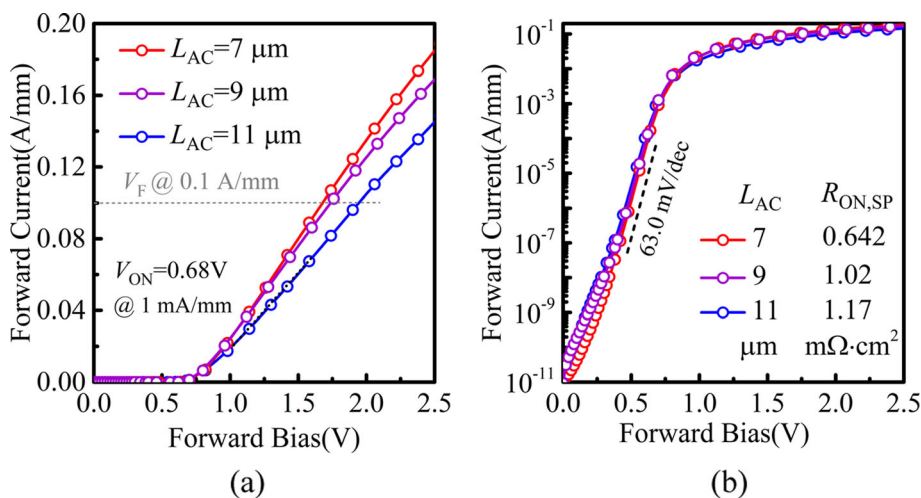


Fig. 4 Measured forward bias I - V characteristics of DJ SBDs in **a** linear and **b** semi-log scale with different L_{AC}

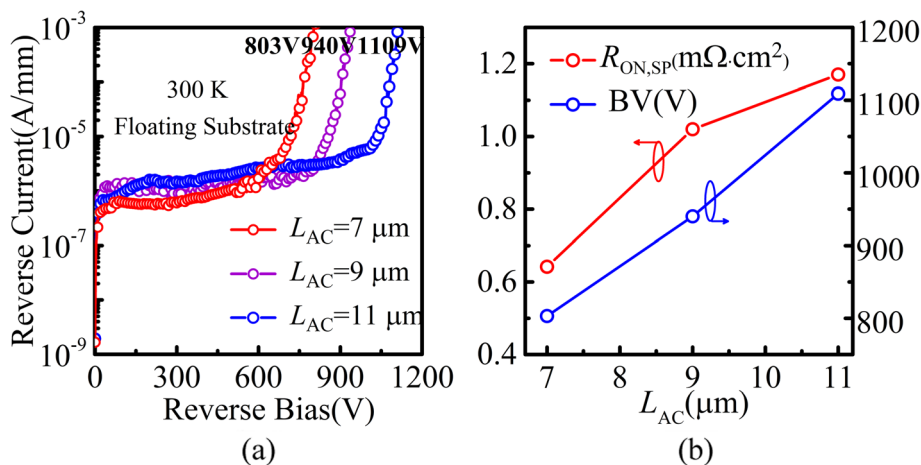


Fig. 5 a Measured reverse blocking I - V characteristics of DJ SBDs with different L_{AC} (b) $R_{ON,SP}$ and BV as the functions of L_{AC}

Schottky contact and electron current path. In addition, the BV decreases slightly with the increase in L_1 because of the shortened drift region. The operation mechanism of the DJ SBDs under forward bias is almost the same as the conventional SBDs, meaning that 2DHG hardly affects the electron current path from the cathode to the anode. With the increasing reverse bias voltage, the 2DEG and 2DHG are fully depleted. There remain fixed positive and negative polarization charges, which forms the polarization junction. As a result, a flat E-field distribution between the cathode and anode is obtained (Fig. 3).

As shown in the Fig. 3, the breakdown characteristic and polarization-junction mechanism were confirmed by 2-D Sentaurus TCAD from Synopsys. We had accounted for several important physical phenomena in simulation, including bandgap narrowing, polarization, electron/hole mobility, impact ionization and SRH recombination.

Hall effect measurement was adopted to determine the 2DHG or 2DEG density and mobility values [22]. The measurements were performed by Van der Pauw method at room temperature. To measure 2DHG according to Ref. [17], Hall measurement samples were fabricated with Ni/Au ohmic contacts. The density and mobility of the 2DHG were $9 \times 10^{12} \text{ cm}^{-2}$ and $15 \text{ cm}^2/\text{V s}$, respectively. The 2DEG was measured by the samples with recessing GaN-top and partially AlGaIn fabricated with Ti/Al/Ni/Au ohmic contacts (for 2DEG). The density and mobility of the 2DEG were $8.5 \times 10^{12} \text{ cm}^{-2}$ and $970 \text{ cm}^2/\text{V s}$, respectively. The Hall measurements showed that the hole mobility was still much lower than the bulk mobility over $100 \text{ cm}^2/\text{V s}$. The degradation of mobility was attributed to the diffusion of Mg from the p-GaN to the undoped GaN during the MOCVD growth.

Results and Discussion

The measured I - V forward characteristics of the SBDs with various L_{AC} are plotted in Fig. 4a and b. The turn-on voltage (V_{ON}) is 0.68 V with a small variation of 0.02 V. The ideality factor and the barrier height of the SBDs are calculated as 1.44 ± 0.15 and $0.76 \pm 0.04 \text{ eV}$, respectively. Figure 4a shows that the high forward current density of 183 mA/mm and 144 mA/mm (@ forward bias of 2.5 V) and the on-resistance of 0.642 and 1.17 $\text{m}\Omega \text{ cm}^2$ are achieved at $L_{AC} = 7$ and 11 μm , respectively. In addition, an excellent on/off current ratio $\sim 10^{10}$ is obtained as shown in Fig. 4b. The subthreshold slope (SS) is 63.0 mV/dec, which is close to the ideal SS (59.6 mV/dec).

Figure 5a shows the measured reverse blocking I - V characteristics of the SBDs with various L_{AC} at 300 K. The breakdown voltage of the devices with different L_{AC} is 803 V, 940 V, and 1109 V, respectively, at a leakage current of 1 mA/mm. The densities of 2DEG and 2DHG are supposed the same during the simulation. However, the experimental results show that the densities of 2DHG ($9 \times 10^{12} \text{ cm}^{-2}$) are slightly higher than those of 2DEG ($8.5 \times 10^{12} \text{ cm}^{-2}$). The difference between the fixed positive and negative polarization charges during the off-state affects the charge balance and thus degrades the breakdown voltage. The influence of the L_{AC} on the BV and the $R_{ON,SP}$ is shown in Fig. 5b. A near linear relationship between BV and L_{AC} is obtained, implying the relative flat lateral E-field in the drift region. Owing to the polarization-junction effect, the device demonstrates a high Baliga's figure-of-merit ($\text{FOM} = \text{BV}^2/R_{ON,SP}$) of $1051 \text{ MW}/\text{cm}^2$ (@ $L_{AC} = 11 \mu\text{m}$).

The etching process is vital to the high-quality Schottky interface and ohmic contact. Figure 6a shows the surface morphology of the recessed trench after the

ICP etching (@ 5 °C) and the TMAH solution. The etch rate is approximately 4.9 nm/min, and the final selected recipe is with a Cl_2 of 4 sccm, an ICP power of 50 W, and an RF power of 15 W. The root mean square (RMS) roughness is 0.244 nm with the scan area of $2 \times 2 \mu\text{m}^2$.

Because the customized epitaxial layer includes 45 nm GaN-top layer and 45 nm AlGaIn layer, the ohmic contact (for 2DEG) process is different from the conventional SBDs. Without recessing both GaN-top and AlGaIn barrier layers, low contact resistance is difficult to be achieved by annealing because of the potential barrier between the ohmic metal and the 2DEG. However, if the barrier is over recessed, the

stress release leads to a reduction in the 2DEG concentration. The extra processes are adopted to reduce the ohmic contact resistance. The surfaces of the samples are treated by the HCl solution to remove native oxide layer before deposition. In addition, the plasma surface treatment is adopted (ICP power 50 W BCl_3 10 sccm 3 min) to introduce surface donor states [24]. Figure 6b demonstrates the dependence of the contact resistance on the trench depth. The optimized depth is obtained from 50 to 55 nm. The high temperature rapid thermal annealing (RTA) for the Ti/Al/Ni/Au contact is investigated in Fig. 6c. The annealing temperature is from 840 to 890 °C, and the 870 °C results in the lowest contact resistance. Annealing at high temperature, i.e., 870 °C, is conducive to the formation of TiN at the Ti/nitride interface. However, higher temperature (e.g., 890 °C) increases the interdiffusion of Au and Al, which is disadvantageous for the formation of good ohmic contacts.

Figure 7a–c exhibit the statistical plots of the static characteristics including V_{ON} , V_{F} , and BV. The data are extracted from 72 SBDs with L_{AC} of 7, 9, and 11 μm fabricated in 3 separate process runs. The devices display stable forward turn-on characteristics and the V_{ON} is independent with L_{AC} because V_{ON} is mainly determined by the Schottky contact. The low-damage ICP etching process, the precisely controlled trench depth, and the high-quality Schottky interface contribute to the excellent uniformity of the V_{ON} and V_{F} . In addition, with the increase in L_{AC} (from 7 to 11 μm), there is a monotonical increase ($\sim 100 \text{ V}/\mu\text{m}$) in the BV observed in proposed structures. Figure 7d shows the histogram statistics of the V_{ON} for 72 devices, and the mean value is 0.68 V with a small standard derivation of 0.02 V.

The temperature dependence of the reverse and forward characteristics is assessed in Fig. 8. As shown in Fig. 8a, an increase in ambient temperature from 300 to 475 K results in an increase in the $R_{\text{ON,SP}}$ by a factor of 1.94.

The dynamic characteristics of the DJ SBDs are measured by Agilent B1505A power device analyzer. The anode pulse quiescent bias points are set to be -10 V, -20 V, -30 V, -40 V, -70 V, and -100 V, with the anode pulse width and period of 0.5 ms/500 ms. Figure 9b shows the dynamic $R_{\text{ON,SP}}$ as a function of the stress voltage. The dynamic $R_{\text{ON,SP}}$ even at 100 V reverse stress voltage is just 1.18 times of the one without reverse stress, which is comparable to Ref. [8]. The limited increase in the dynamic $R_{\text{ON,SP}}$ contributes to the reduction in interface state. The degradation of dynamic $R_{\text{ON,SP}}$ needs further work.

Figure 10 presents the benchmark plot of BV versus $R_{\text{ON,SP}}$ for GaN power diode on Si/SiC/sapphire substrates [8, 10, 22, 25–31]. The proposed device with L_{AC}

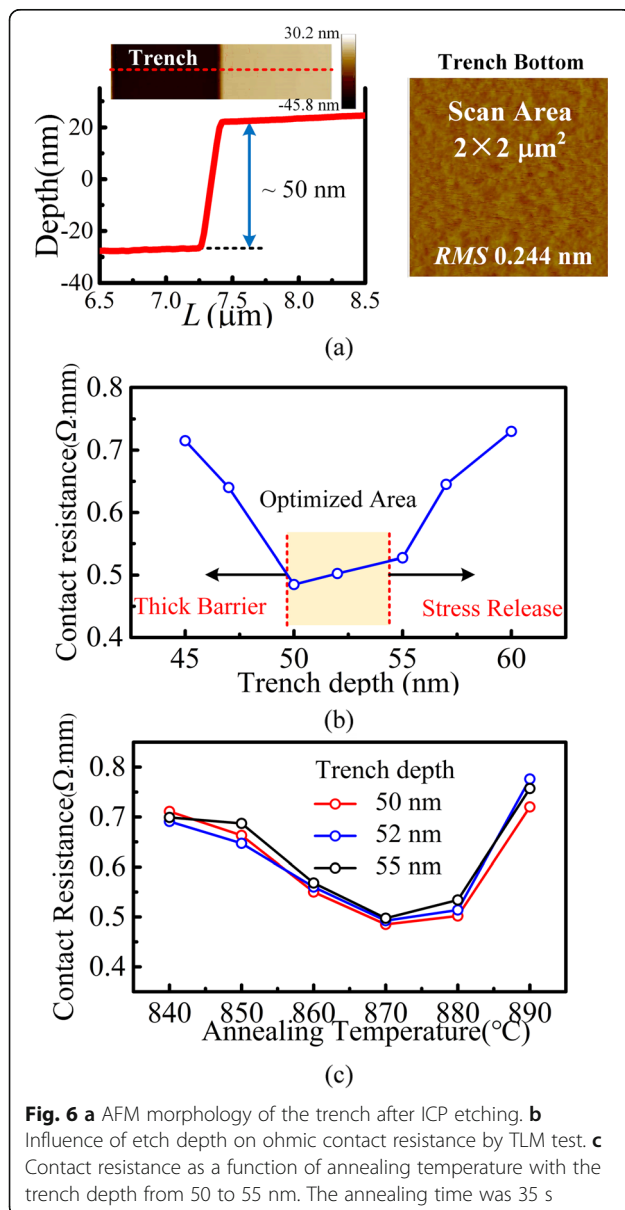


Fig. 6 a AFM morphology of the trench after ICP etching. b Influence of etch depth on ohmic contact resistance by TLM test. c Contact resistance as a function of annealing temperature with the trench depth from 50 to 55 nm. The annealing time was 35 s

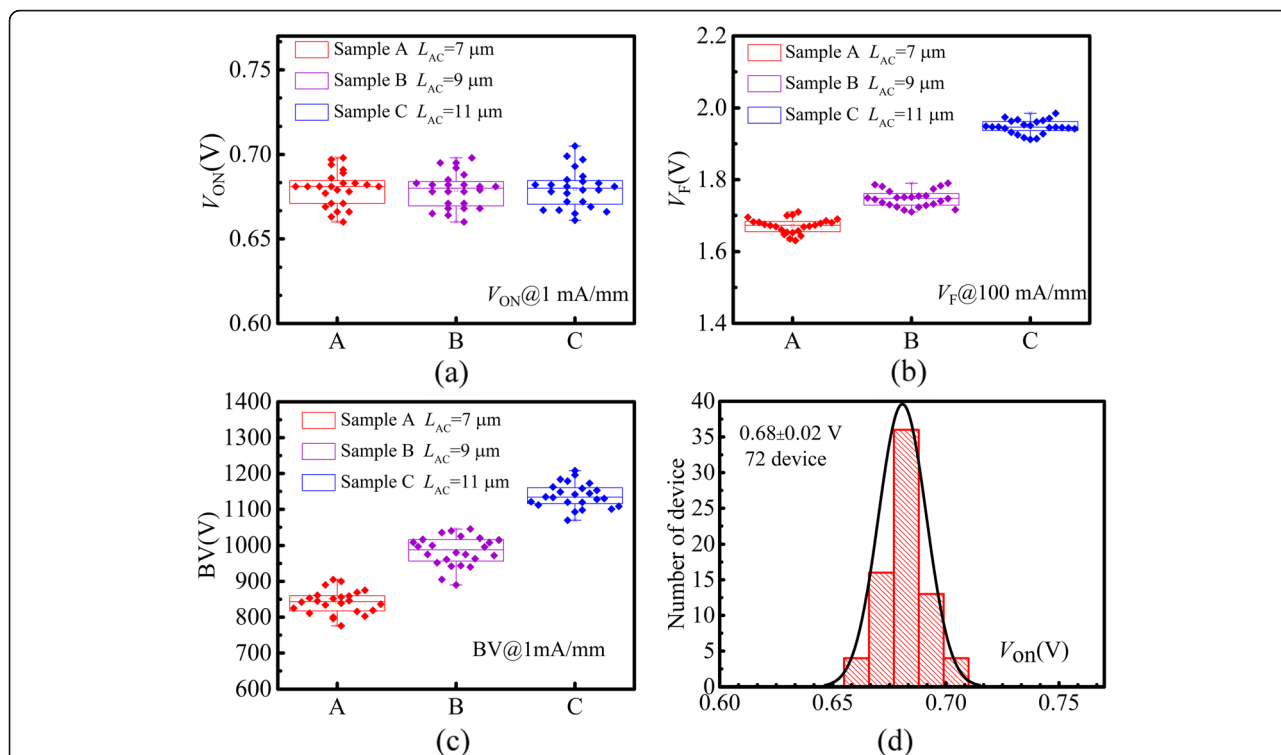


Fig. 7 Statistical plots of **a** turn-on voltage, **b** forward voltage, and **c** breakdown voltage extracted from 72 SBDs with L_{AC} of 7, 9, and 11 μm fabricated in 3 separate process runs. **d** Distribution of V_{ON} for 72 devices

of 11 μm demonstrates a BV of 1109 V with a corresponding $R_{ON,SP}$ of 1.17 $\text{m}\Omega\text{cm}^2$, leading to a high Baliga’s FOM of 1051 MW/cm^2 . This value is the best results among the lateral GaN power diode on Si substrate.

Conclusion

A double-heterojunction GaN/AlGaIn/GaN-on-Si SBD with a high figure of merit is fabricated. The low-

damage ICP etching process results in the optimized ohmic and Schottky contacts for the proposed device. Therefore, a low V_{ON} of 0.68 V with good uniformity and a low $R_{ON,SP}$ of 1.17 $\text{m}\Omega\text{cm}^2$ are obtained in the device with L_{AC} of 11 μm . A high Baliga’s FOM of 1051 MW/cm^2 is achieved due to the polarization-junction effect. The high performance together with the low-cost GaN-on-Si technology exhibits great potential for future power applications.

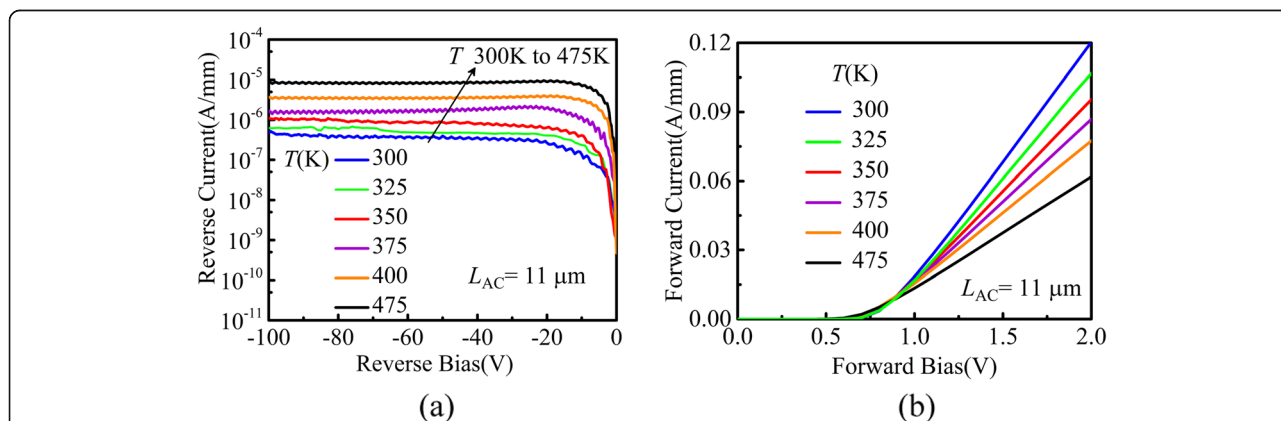
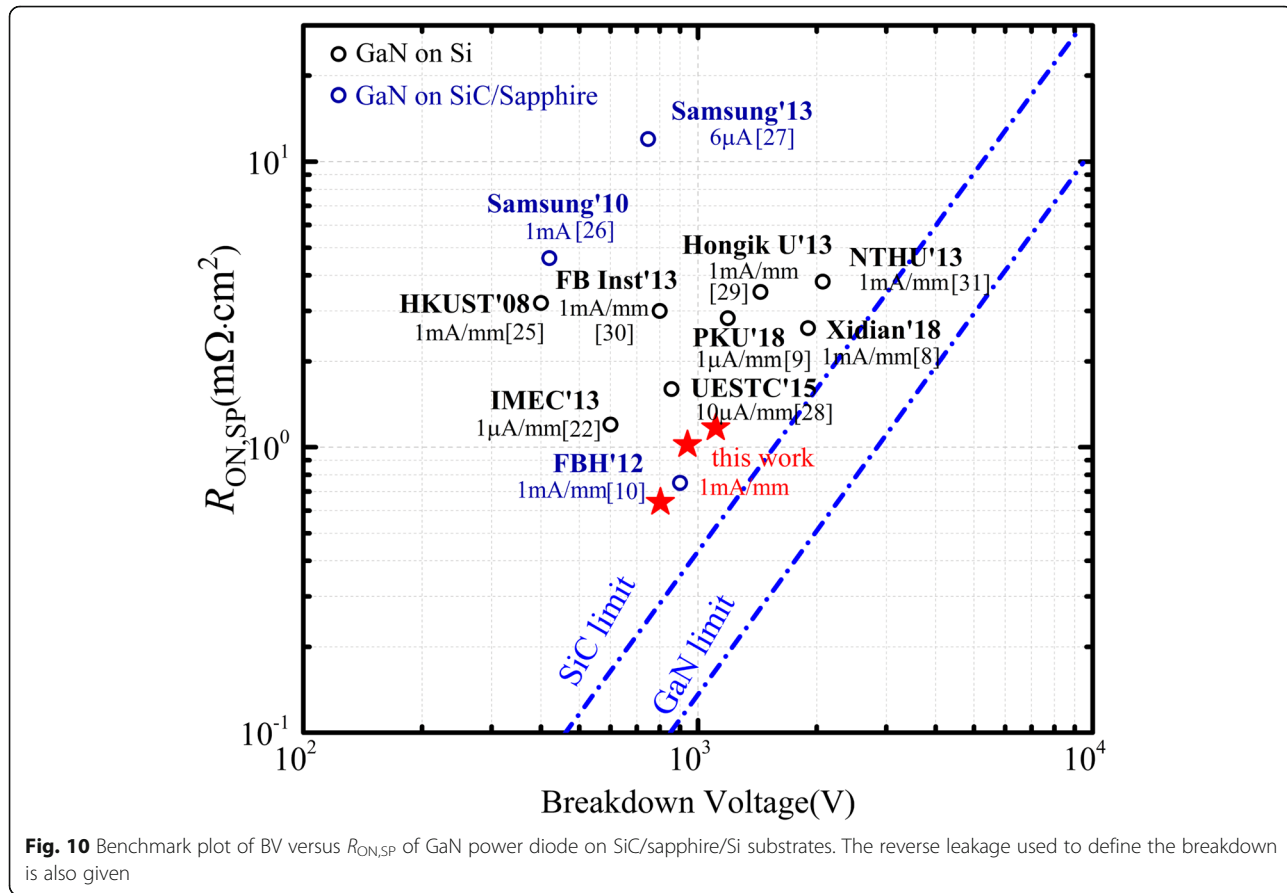
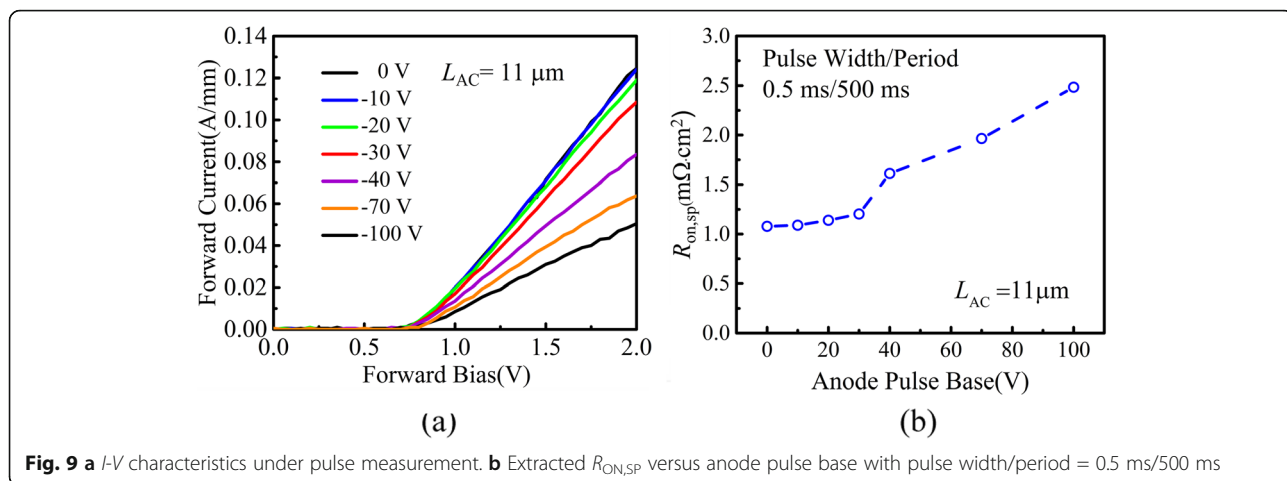


Fig. 8 a Reverse leakage current and **b** forward characteristics for the DJ SBDs at different temperatures



Abbreviations

SBD: Schottky barrier diode; 2DEG/2DHG: Two-dimensional electron/hole gas; MOCVD: Metal-organic chemical vapor deposition; ICP: Inductively coupled plasma; TEM: Transmission electron microscope; AFM: Atomic force microscope; BV: Breakdown voltage; $R_{ON,SP}$: Specific on-resistance; V_{ON} : Turn-on voltage; FOM: Figure-of-merit

Acknowledgements

Not applicable

Authors' Contributions

Tao Sun conceived and performed the experiments and the data analysis. Xiaorong Luo supervised this work. All authors discussed the results and contributed to the final manuscript. The authors read and approved the final manuscript.

Funding

This work was supported by the National Natural Science Foundation of China under Grant 51677021 and 61874149, the Outstanding Youth Science and Technology Foundation of China under Grant 2018-JCJQ-ZQ-060, and the stable support project for the institutes of Basic scientific research 1902 N261.

Availability of Data and Materials

All data generated or analyzed during this study are included in this article.

Competing Interests

The authors declare that they have no competing interests.

Received: 11 April 2020 Accepted: 29 June 2020

Published online: 16 July 2020

References

- Mishra UK, Parikh P, Wu YF (2002) AlGaIn/GaN HEMTs—an overview of device operation and applications. *Proc IEEE* 90:1022
- Chow TP, Tyagi R (1994) Wide bandgap compound semiconductors for superior high-voltage unipolar power devices. *IEEE TED* 41:1481
- Wu YF, Kapolnek D, Ibbetson JP, Parikh P, Keller BP, Mishra UK (2001) Very-high power density AlGaIn/GaN HEMTs. *IEEE TED* 48:586
- Tsou CW, Wei KP, Lian YW, Shawn S, Hsu H (2016) 2.07-kV AlGaIn/GaN Schottky barrier diodes on silicon with high Baliga's figure-of-merit. *IEEE TED* 37:70
- Zhu M, Song B, Qi M, Hu Z, Nomoto K, Yan X, Cao Y, Johnson W, Kohn E, Jena D, Xing H (2015) 1.9-kV AlGaIn/GaN lateral Schottky barrier diodes on silicon. *IEEE EDL* 36:375
- Kang X, Wang X, Huang S, Zhang J, Fan J, Yang S, Wang Y, Zheng Y, Wei K, Zhi J, Liu X (2018) Recess-free AlGaIn/GaN lateral Schottky barrier controlled Schottky rectifier with low turn-on voltage and high reverse blocking. *Proc ISPSD*:280
- Han S, Yang S, Sheng K (2018) High-Voltage and High-I/V Vertical GaN-on-GaN Schottky Barrier Diode With Nitridation-Based Termination. *IEEE EDL* 39:572
- Zhang T, Zhang J, Zhou H, Chen T, Zhang K, Hu Z, Bian Z, Dang K, Wang Y, Zhang L, Ning J, Ma P, Hao Y (2018) A 1.9-kV/2.61-m Ω -cm Lateral GaN Schottky Barrier Diode on Silicon Substrate With Tungsten Anode and Low Turn-ON Voltage of 0.35 V. *IEEE EDL* 39:1548
- Gao J, Jin Y, Xie B, Wen C, Hao Y, Shen B, Wang M (2018) Low ON-Resistance GaN Schottky Barrier Diode With High VON Uniformity Using LPCVD Si N Compatible Self-Terminated, Low Damage Anode Recess Technology. *IEEE EDL* 39:859
- Bahat-Treidel E, Hilt O, Zhytnytska R, Wentzel A, Meliani C, Wurfl J, Trankle G (2012) Fast-switching GaN-based lateral power Schottky barrier diodes with low onset voltage and strong reverse blocking. *IEEE EDL* 33:357
- Saitoh Y, Sumiyoshi K, Okada M, Horii T, Miyazaki T, Shiomi H, Ueno M, Katayama K, Kiyama M, Nakamura T (2010) Extremely low on-resistance and high breakdown voltage observed in vertical GaN Schottky barrier diodes with high-mobility drift layers on low-dislocation-density GaN substrates. *APE* 3:8
- Unni V, Long H, Sweet M, Balachandran A, Narayanan EM, Nakajima A, Kawai H (2014) 2.4 kV GaN polarization superjunction Schottky barrier diodes on semi-insulating 6H-SiC substrate. *Proc ISPSD*:245
- Lee CH, Lin WR, Lee YH, Huang J (2018) Characterizations of enhancement-mode double heterostructure GaN HEMTs with gate field plates. *IEEE TED* 65:488
- Tang K, Li Z, Chow TP, Niiyama Y, Nomura T, Yoshida S (2009) Enhancement-mode GaN hybrid MOS-HEMTs with breakdown voltage of 1300V. *Proc ISPSD*:279
- Nakajima A, Dhyani MH, Narayanan EMS, Sumida Y, Kawai H (2011) GaN based Super HFETs over 700V using the polarization junction concept. *Proc ISPSD*:280
- Nakajima A, Unni V, Menon KG, Dhyani MH, Narayanan EMS, Sumida Y, Kawai H (2012) GaN-based bidirectional super HFETs using polarization junction concept on insulator substrate. *Proc ISPSD*:265
- Kawai H, Yagi S, Nakamura F, Saito T, Kamiyama Y, Yamamoto A, Amano H, Unni V, Narayanan EMS (2017) Low cost high voltage GaN polarization superjunction field effect transistors. *Phys Status Solidi A* 214:1600834
- Nakajima A, Sumida Y, Dhyani MH, Kawai H, Narayanan EM (2011) GaN-based super heterojunction field effect transistors using the polarization junction concept. *IEEE EDL* 32:542
- Chen KJ, Häberlen O, Lidow A, Tsai CL, Ueda T, Uemoto Y, Wu YF (2017) GaN-on-Si power technology: Devices and applications. *IEEE TED* 64:779
- Meneghini M, Meneghesso G, Zanoni E (2017) *Power GaN Devices*. Springer International Publishing, Cham
- Lenci S, De Jaeger B, Carbonell L, Hu J, Mannaert G, Wellekens D, You S, Bakeroort B, Decoutere S (2013) Au-free AlGaIn/GaN power diode on 8-in Si substrate with gated edge termination. *IEEE EDL* 34:1035
- Nakajima A, Sumida Y, Dhyani MH, Kawai H, Narayanan EM (2010) High density two-dimensional hole gas induced by negative polarization at GaN/AlGaIn heterointerface. *APE* 3:121004
- Kim KW, Jung SD, Kim DS (2011) Effects of TMAH Treatment on Device Performance of Normally Off Al O /GaN MOSFET. *IEEE EDL* 32:10
- Fujishima T, Joglekar S, Piedra D, Lee K, Uedono A, Palacios T (2013) Formation of low resistance ohmic contacts in GaN-based high electron mobility transistors with BCl surface plasma treatment. *APL* 103:083508
- Chen W, Wong KY, Huang W, Chen KJ (2008) High-performance AlGaIn/GaN lateral field-effect rectifiers compatible with high electron mobility transistors. *APL* 92:253501
- Lim W, Jeong JH, Lee JH, Hur SB, Kim KS, Song SY, Yang JI, Pearton SJ (2010) Temperature dependence of current-voltage characteristics of Ni–AlGaIn/GaN Schottky diodes. *APL* 97:242103
- Lee JH, Park C, Im KS, Lee JH (2013) AlGaIn/GaN-based lateral-type Schottky barrier diode with very low reverse recovery charge at high temperature. *IEEE TED* 60:3032
- Zhou Q, Jin Y, Shi Y, Mou J, Bao X, Chen B, Zhang B (2015) High reverse blocking and low onset voltage AlGaIn/GaN-on-Si lateral power diode with MIS-gated hybrid anode. *IEEE EDL* 36:660
- Lee JG, Park BR, Cho CH, Seo KS, Cha HY (2013) Low turn-on voltage AlGaIn/GaN-on-Si rectifier with gated ohmic anode. *IEEE EDL* 34:214
- Treidel EB, Hilt O, Wentzel A, Wurfl J, Trankle G (2013) Fast GaN based Schottky diodes on Si (111) substrate with low onset voltage and strong reverse blocking. *Phys Status Solidi C* 10:849
- Lian YW, Lin YS, Yang JM, Cheng CH, Shawn SHH (2013) AlGaIn/GaN Schottky barrier diodes on silicon substrates with selective Si diffusion for low onset voltage and high reverse blocking. *IEEE EDL* 34:981

Publisher's Note

Springer Nature remains neutral with regard to jurisdictional claims in published maps and institutional affiliations.